Neuroprotective and anticancer effects of 7-Methoxyheptaphylline via the TAK1 pathway

CHANTANA BOONYARAT[1], MONGKHONPHAN TANTIWATCHARAKUNTHON[2], PITCHAYAKARN TAKOMTHONG[1], CHAVI YENJAI[3], YOSHIHIRO HAYAKAWA[4], PORNNGARM DEJKRIENGKRAIKUL[5,6], SUCHADA CHAIWIWATRAKUL[7] and PORNTHIP WAIWUT[2]

[1]Faculty of Pharmaceutical Sciences, Khon Kaen University, Khon Kaen 40002; [2]Faculty of Pharmaceutical Sciences, Ubon Ratchathani University, Ubon Ratchathani 34190; [3]Natural Products Research Unit, Department of Chemistry and Center of Excellence for Innovation in Chemistry, Faculty of Science, Khon Kaen University, Khon Kaen 40002, Thailand; [4]Section of Host Defences, Institute of Natural Medicine, University of Toyama, Toyama 930-0194, Japan; [5]Department of Biochemistry, Faculty of Medicine, Chiang Mai University; [6]Excellent Center for Research and Development of Natural Products for Health, Chiang Mai University, Chiang Mai 50200; [7]Department of English, Faculty of Humanities and Social Sciences, Ubon Ratchathani Rajabhat University, Ubon Ratchathani 34000, Thailand

Received May 6, 2022; Accepted October 24, 2022

DOI: 10.3892/or.2022.8452

Abstract. 7-Methoxyheptaphylline (7-MH) is a carbazole extracted from *Clausena harmandiana*, a medicinal plant that is used to treat headaches and stomachaches. The aim of the present study was to examine the neuroprotective effects and anticancer activity of 7-MH. Cell death was assessed using an MTT assay and flow cytometry. The expression of apoptosis-related proteins was determined by western blot analysis. An animal model was used to test anti-metastasis. The interactions between 7-MH and the molecular target were observed using molecular docking. The results revealed that 7-MH provided protection against hydrogen peroxide (H_2O_2)-induced neuronal cell death. In cancer cells, 7-MH induced SH-SY5Y, 4T1, HT29, HepG2, and LNCaP cell death. 7-MH inhibited metastasis of HT29 cells *in vitro* and 4T1-Luc cells *in vitro* and *in vivo*. 7-MH inhibited proteins, including P-glycogen synthase kinase (GSK)-3, and cleaved caspase-3, but it activated anti-apoptotic proteins in H_2O_2-induced SH-SY5Y cell death. By contrast, 7-MH activated the cleaving of caspase-3 and GSK-3, but it suppressed anti-apoptotic proteins in SH-SY5Y cells. 7-MH reduced the levels of NF-κB and STAT3 in 4T1 cells; phospho-p65, Erk, and MAPK13 in LNCaP cells; and phospho-Erk and matrix metalloproteinase-9 in HT29 cells. Molecular docking analysis showed that 7-MH targets TAK1 kinase. The present study indicated that 7-MH induced apoptosis of cancer cells and provided protection against H_2O_2-induced neuron cell death via TAK1 kinase.

Correspondence to: Dr Pornthip Waiwut, Faculty of Pharmaceutical Sciences, Ubon Ratchathani University, 85 Sathonlamark Road, Warin Chamrap, Ubon Ratchathani 34190, Thailand
E-mail: pontip.w@ubu.ac.th

Key words: 7-methoxyheptaphylline, *Clausena harmandiana*, cancer, neuron cells, TGF-β-activated kinase 1, glycogen synthase kinase-3, apoptosis

Introduction

Cancer and Alzheimer's disease (AD) have become leading causes of death worldwide (1). Previous studies have identified relationships between cancer and AD in which the amyloid precursor protein (APP) plays an important role. APP is a transmembrane protein, source of β-amyloid aggregation which is one of the major causes of AD, is expressed in various neuron cells and may be involved in development of cells (2,3). In cancer cells, it has been reported that APP is a primary androgen-responsive gene, found in breast and prostate cancer; it is also implicated in various human cancers including colon, lung, breast, parathyroid, prostate, thyroid and breast cancers, and its high immunoreactivity is related with poor prognoses for prostate cancer and estrogen-receptor-positive breast cancer patients (4-10). Therefore, APP may enhance the growth and metastasis of prostate cancer cells by regulating the expression of metalloproteinase and EMT-related genes (11). It has been observed that APP increases expression and processing in pancreatic cancer. This molecule also promotes growth in pancreatic cancer cells through undergoing proteolytic processing to release a soluble NH2-terminal ectodomain fragment (sAPP) (12). Moreover, a relationship between reactive oxygen species (ROS) and androgen receptor (AR) has been identified; as well as the mechanisms of AR activation through oxidative stress including AR overexpression, AR co-regulators or intracellular signal transduction pathways, increasing of AR mutations or splice variants, and *de novo* androgen synthesis. AR signaling activated by oxidative stress may contribute to survival and evading to apoptosis in prostate cancer cells in response to androgen deprivation therapy (13).

Prostate tumors characterized by androgen receptor (AR) expression and signaling pathways in processes of carcinogenesis, development, and progression (14). Conversely, androgen deprivation therapy, which decreases androgen level, and interferes with AR function, is gold-standard treatment of prostate cancer (15).

ROS, including superoxide (O_2^-), hydrogen peroxide (H_2O_2), and hydroxyl radicals (HO•) which are produced by the partial reduction of oxygen, comprise an important mechanism of AD. In the process of mitochondrial oxidative phosphorylation, ROS are endogenously produced in the cells, or can be generated exogenously from xenobiotic compounds when cellular antioxidant defense system is overcome by increase in ROS or a decrease in cellular antioxidant ability. The oxidative stress can induce the damage of biomolecules (nucleic acids, proteins and lipids) which is a leading cause of various disorders including carcinogenesis (16), neurodegenerative diseases (17), atherosclerosis, diabetes (18), and aging (19). Moreover, oxidative stress can regulate various cellular reactions, including AR signaling, through direct or indirect reactions (20). Oxidative stress has been shown to be involved in the tumorigenesis and transformation of prostate cancer (21-23) as well as in the conversion of androgen-dependent prostate cancer into CRPC (22,24,25). Together, these results indicated the cross-talk relation between oxidative stress and AR signaling.

Transforming growth factor-β (TGF-β)-activated kinase 1 (TAK1), is a serine/threonine kinase in the mitogen-activated protein kinase (MAP3K) family. TAK1 is the central core for various signaling pathways and it was originally recognized as a transforming growth factor-β-activated kinase and was demonstrated to phosphorylate and activate various downstream target proteins and promote cancer. After stimulation by specific ligands, IL and TGFβ receptors enhance the activation of TRAF6, and E3 ubiquitin ligase mediates the activation of TAK1. Active TAK1 mediates the processes of cancer cells including proliferation, survival and resistance to chemotherapy through NF-κB activation, triggering additional signaling pathways including p38, JNK, and acting on different transcription factors (TFs). Previous studies demonstrated that targeting the TAK1 kinase activity dramatically induced apoptosis and increased sensitivity to chemotherapy and radiotherapy of cancer cells (26-29). Glycogen synthase kinase (GSK)3 is a serine/threonine kinase that consists of 2 genes, GSK-3α and GSK-3β. GSK-3 has been involved in a number of human cancers, including pancreatic cancer. In distinct, a recent study demonstrated that GSK-3α interacts with TAK1 which stabilizes the TAK1-TAB complex. This enhances noncanonical NF-kB activation in pancreatic cancer cells. The suppression of GSK-3 results in a significant reduction of TAK1 levels. Different from other kinases, when dephosphorylated GSK-3β which is active form, promotes inflammation and apoptosis. In opposition, increased phosphorylation reduced GSK-3β activity. GSK-3β suppression has beneficial effects on memory in other disease models. GSK-3β controls TAK1 pathways. Suppression of GSK-3β was neuroprotective and ameliorated stroke-induced cognitive impairments. TAK1 is an upstream regulator of GSK-3β. Targeting GSK-3β could be a novel therapeutic strategy for cognitive deficits (30).

Clausena harmandiana (*C. harmandiana*) or 'Song fa' in Thai is a medicinal plant, used for the treatment of headaches, and illness stomachaches (31). It has been found that the roots of *C. harmandiana* plant consist of carbazole and coumarins alkaloids (32). Carbazoles and coumarins alkaloids have been isolated and evaluated for their pharmacological activities including, antimalarial, anti-tuberculosis, and antifungal properties. In a previous study by the authors, it was revealed that the major components in *C. harmandiana* were heptaphylline and 7-methoxyheptaphylline (7-MH), which exhibited anticancer activities against NCI-H187 and KB cell lines (33). Moreover, 7-MH (Fig. 1) showed a neuroprotective effect against H_2O_2-induced cell death of NG108-15 cells (34). In order to search for new drug for cancer and anti-AD prevention and treatment with high efficacy, low toxicity, and decrease side effects, the present study investigated the antiapoptotic effects of H_2O_2-induced oxidation of 7-MH on SH-SY5Y neuroblastoma cells and the apoptotic effects of 7-MH on SH-SY5Y neuroblastoma cells and LNCaP prostate cancer cells. To clarify the mechanism of action of 7-MH, the effect of 7-MH on signaling proteins involved in the TAK1-mediated apoptosis pathway including GSK-3, MAPK13, anti-apoptotic proteins and pro-apoptotic proteins in cancer and Alzheimer's model, was investigated.

Materials and methods

Cell culture. SH-SY5Y (neuroblastoma cell line) (CRL-2266), HepG2 (liver cancer cells) (HB-8065), HT29 (colorectal cancer cells) (HTB-38), and 4T1 (breast cancer cells) (CRL-2539) were purchased from the American Type Culture Collection (ATCC) and authenticated using short tandem repeat analysis (also conducted by the ATCC). The cells were maintained in Eagle's minimum essential medium (Gibco; Thermo Fisher Scientific, Inc.) supplemented with 10% fetal bovine serum (Amresco, LLC), 100 units/ml penicillin and 100 μg/ml streptomycin (Gibco; Thermo Fisher Scientific, Inc.) at 37˚C in 5% CO_2. LNCaP cell were maintained in RPMI-1640 (Gibco; Thermo Fisher Scientific, Inc.) supplemented with 10% fetal calf serum, 100 units/ml penicillin, and 100 μg/ml streptomycin at 37˚C in 5% CO_2.

Cell cytotoxicity assay. SH-SY5Y cells, HepG2, HT29, 4T1, and LNCaP cells were plated in 96-well microplates at $4x10^5$ cells/wells and then incubated for 48 h. Cells were treated with 7-MH at different concentrations and reference compound for 24, 48 and 72 h. Then, 10 μl of MTT reagent (5 mg/ml) (Sigma-Aldrich; Merck KGaA) was added. The cells were incubated for 2 h until purple precipitate was visible after addition of dimethyl sulfoxide. The absorbance at 570 nm was measured. The percentage calculation of cell viability was carried out using the following formula: % Cell viability=(Absorbance of treated cells x100)/Absorbance of control (untreated cells). Cell morphology was examined using a phase-contrast microscope by having 36 μM doxorubicin (Sigma-Aldrich) as positive control.

Neuroprotective effect. SH-SY5Y cells were plated in 96-well microplates at a density $4x10^5$ cells/wells and then incubated for 48 h. The cells were treated with various concentrations

of 7-MH or 100 μM NAC for 2 h. Then, the cells were treated with 250 μM H_2O_2 for 4 h to induce oxidative stress. Cell viability was determined by MTT colorimetry. Absorbance was measured at 570 nm.

Fluorescence-activated cell-sorting (FACS) analysis. Apoptosis occurs as a result of G0/G1 phase arrest. Apoptosis as a protective mechanism ensures homeostasis of host cells through cell shrinkage, fragmentation of cellular DNA and formation of 'apoptotic bodies' subsequently leading to cell death. For cell cycle analysis, the cells were treated with various concentrations of 7-MH for 2 h. Then, the cells were treated with H_2O_2 for 4 h to induce oxidative stress. The cells were fixed by ethanol for 2 h at 4˚C and stained with 50 mg/ml propidium iodide (PI) for 30 min in the presence of RNase before analysis. The percentage of apoptotic cells was quantitated using an FACScan flow cytometer with BD FACSDivaTM software (v. 6.1.3) (BD FACSAria; BD Biosciences). Late apoptotic cells were distinguished from non-apoptotic, intact cells by their decreased DNA content, which was determined by their low PI staining intensity.

Preparation of cell extracts. In order to investigate the mechanisms of interaction with the apoptotic pathway in cancer cells, the cells were plated in six-well plates at a density of $1x10^6$ cells/wells and then incubated for 48 h. The cells were treated with various concentrations of 7-MH at 30 min, and cell death was induced with H_2O_2 at 15 min for SH-SY5Y cells. In HepG2, HT29, 4T1, and LNCaP cells, the cells were treated with various concentrations of 7-MH at the indicated time. Whole-cell lysates were prepared with lysis buffer [25 mM HEPES, pH 7.7, 0.3 mM $MgCl_2$, 0.2 mM EDTA, 10% Triton X-100, 20 mM β-glycerophosphate, 1 mM sodium orthovanadate, 1 mM phenylmethylsulfonyl fluoride (PMSF), 1 mM dithiothreitol (DTT), 10 μg/ml aprotinin, and 10 μg/ml leupeptin] (Gibco; Thermo Fisher Scientific, Inc.). The cell lysates were collected from the supernatant after centrifugation at 2,500 x g for 10 min 4˚C.

Immunoblotting. The total protein concentration was measured by using the Bradford dye-binding method (Bio-Rad). The cell lysates (15 μl)were loaded and resolved by 7.5-12.5% SDS-PAGE and transferred to an Immobilon-P-nylon membrane (MilliporeSigma). The membrane was treated with BlockAcc (Dainippon Phamaceutical Co., Ltd.) and probed at room temperature for 2 h with the following primary antibodies: anti-caspase-3 (cat. no. 9662), GSK-3 (cat. no. 5558), phospho-p38 (cat. no. 4511), p38 (cat. no. 54470), Mcl-1 (cat. no. 94296), Bcl-xL (cat. no. 2764), BAX (cat. no. 5023), phospho-Akt (cat. no. 4060), Akt (cat. no. 4691), phospho-ERK (cat. no. 9911), phospho-P65 (cat. no. 3031), P65 (cat. no. 3033), Bcl-2 (cat. no. 4223), survivin (cat. no. 2808), MAPK13 (cat. no. 4511), and anti-actin antibodies (cat. no. 3700), all diluted at 1:1,000 and obtained from Cell Signaling Technology, Inc. The antibodies were detected using horseradish peroxidase-conjugated anti-rabbit (cat. no. 14708), anti-mouse (cat. no. 14709), and anti-goat IgG (cat. no. 98164) secondary antibodies (1: 5,000; Cell Signaling Technology, Inc.) and visualized using the enhanced chemiluminescence system (Life Science Technology). Densitometric analysis of western blot bands was performed using ImageJ software (version IJ 1.46 r; National Institutes of Health.).

Migration and invasion assays. The cancer cell migration and invasion capacities were determined using a Transwell assay. A total of $1x10^6$ cells/well in serum-free DMEM were added into the top chambers of a 24-well insert (pore size, 8-mm; Corning Life Sciences) and incubated for 4 h to allow the cells to attach. The cells were treated with candidone and incubated for 24 h at 37˚C. For the invasion assays, the membranes were pre-coated with collagen for 4 h at 37˚C. The lower chambers were filled with DMEM supplemented with 10% fetal bovine serum as a chemoattractant. After 4 h, the migratory/invasive cells were fixed with a 10% formalin solution at room temperature for 30 min and then stained with 0.05% crystal violet solution at room temperature for 30 min, after which the stained cells were counted under an inverted light microscope (magnification, x20).

Luciferase assay. 4T1 cells were transfected with a luciferase reporter plasmid (Promega Corporation) using Lipofectamine® 2000 (Invitrogen; Thermo Fisher Scientific, Inc.) under the control of NF-κB and STAT3 sites containing a neo-resistance gene. The luciferase activity of transfected cells was compared with 4T1 CMV control cell (the 4T1 cells stably expressing luciferase with a CMV-promoter). A stable clone was isolated in medium containing 500 μg/ml G418 (Thermo Fisher Scientific, Inc.). Cells were seeded in a 96-well plate and treated with DMSO (control) and 0.1, 1, 10, or 100 μM of 7-MH for 24 h and compared with resveratrol as a positive control. Luciferase activity was measured using the Dual-Luciferase reporter assay system (Promega Corporation).

Animal model. Female BALB/c mice (6 weeks old) were separated into groups of 6-7 mice at temperature and humidity of 23±2˚C and 50±10%, respectively, and were administered food and water *ad libitum*. The experiment was carried out according to the standard guidelines of the National Institutes of Health and was approved (approval no. A2017INM-7) by the Animal Care and Use Committee of the University of Toyama (Toyama, Thailand). The lung metastasis model was performed by culturing mouse mammary carcinoma 4T1 cells with the luciferase gene (4T1-Luc2 cells), and then the cells were harvested and resuspended in cold phosphate-buffered saline (PBS). The cell suspensions ($5x10^5$/50 μl/mouse) were inoculated in mice by intravenous injection (the number of mice was n=6 each group and repeated twice so at least 24 mice as total from 30 prepared mice). After 6 days, D-luciferin (150 mg/kg) was injected, and 20 min later, the lungs were harvested from the mice. Lung luminescence was then determined using an imaging system (IVIS Spectrum; Caliper Life Science). The method of euthanasia was cervical dislocation and death was confirmed before disposal of the animal by evaluating consciousness including lack of a heartbeat, lack of respiration, lack of corneal reflex and presence of rigor mortis. In accordance with the Guide for the Care and use of Laboratory Animals of the National Institutes of Health, the humane endpoint was set based on the percentage of body weight loss (20% body-weight reduction).

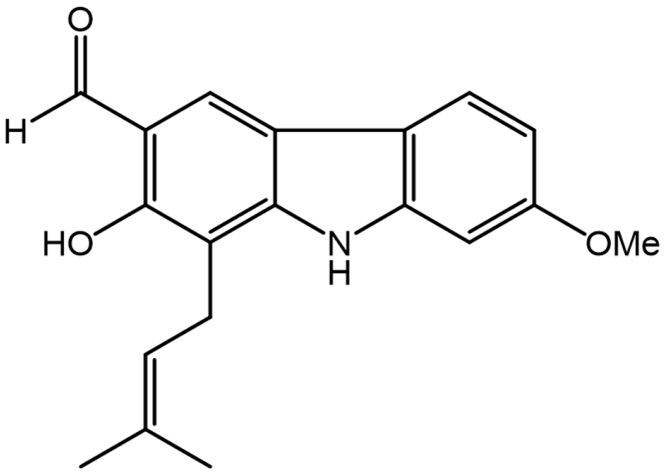

Figure 1. Structure of 7-methoxyheptaphylline.

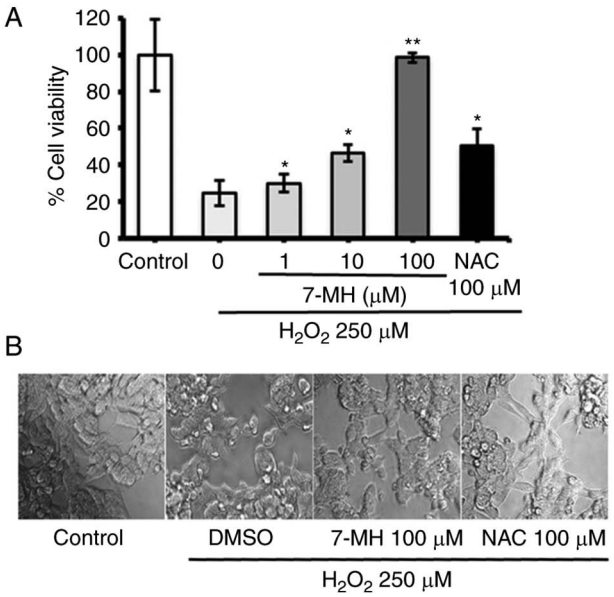

Figure 2. Neuroprotective effect of 7-MH on H_2O_2-induced cell death in neuronal cells. (A) Neuronal cells were treated with various concentrations of 7-MH and 100 μM NAC (reference compound) for 2 h, and cell death was induced via treatment with an H_2O_2 concentration of 250 μM for 4 h. MTT assay was performed on cell viability. (B) The morphology of neuronal cells after 2 h of treatment with 100 μM of 7-methoxyheptaphylline and 100 μM NAC (reference compound), and cell death was induced via treatment with a H_2O_2 concentration of 250 μM for 4 h. Morphological studies were performed using phase contrast microscopy. *P<0.05 and **P<0.01. 7-MH, 7-methoxyheptaphylline.

Molecular docking study. The TAK1 kinase template was prepared from 4GS6 and validated by redocking with the irreversible inhibitor (5Z)-7-oxozeaenol. All hydrogens were added, water molecules were deleted, and Gasteiger charges were assigned to the TAK1 kinase template and all ligands by using AutoDockTools (ADT). The AutoGrid was used to generate grid maps. The grids were designated to include the active site of TAK1 kinase. The grid box dimensions were defined as 100x100x100 Å, and the grid spacing was set to 0.375 Å. All ligands were docked using the Lamarckian genetic algorithm via the Autodock 4.2.6 auxiliary program. The Lamarckian genetic algorithm protocol was set to a population size of 150 individuals with 150 ligand orientation runs. Additionally, the energy evaluation was 1,000,000, which was as the maximum number of evaluations. The docking complex poses were analyzed for their interactions by using BIOVIA Discovery Studio 2017.

Statistical analysis. The statistical technique used for the analysis was a one-way analysis of variance (ANOVA) followed by Tukey's post hoc test for comparison between 2 groups and between 3 or more groups. The data were analyzed using SPSS software (version 24; IBM Corp.). The analysis was performed in triplicate, and the values are presented as the mean ± SDs. P<0.05 was considered to indicate a statistically significant difference.

Results

The neuroprotective effect of 7-MH on H_2O_2-induced apoptosis in SH-SY5Y cells via GSK-3. To investigate the effect of 7-MH on H_2O_2-induced neuronal cell death, neuronal cells were treated with various concentrations of 7-MH or 100 μM NAC (reference compound) for 2 h before switching to 250 μM H2O2 for 4 h. Cell viability was assessed using MTT assay. The results showed significantly increased cell viability when compared with H_2O_2-insulted samples. The values obtained with 7-MH treatment at a concentration of 100 μM showed a stronger neuroprotective effect than that achieved by NAC treatment (Fig. 2A). A decrease in morphologically-confirmed cell death was observed as a result of 7-MH, compared with 100 μM NAC (Fig. 2B). In consistency with previous findings, 7-MH showed a neuroprotective effect on NG108-15 cells (mouse neuroblastoma and rat glioma cell lines) (35).

To verify the 7-MH inhibition of apoptosis by H_2O_2, the cells were labeled with PI and analyzed using flow cytometry (There was a limitation to stain with Annexin V). The results revealed the DNA content histograms obtained after the PI staining of cells that had been treated with various concentrations of 7-MH for 2 h and had been eliminated by treatment with an H_2O_2 concentration of 250 μM for 4 h. When the cells were incubated in the medium alone (control), a single peak of nuclei with diploid DNA content was observed. By contrast, when the cells were incubated in H_2O_2 alone (negative control), an increase in apoptotic cells in sub-G_0/G_1 was observed. When the cells were incubated in NAC and H_2O_2 (positive control), the results were similar to those of the control group. In the presence of 7-MH, inhibiting apoptosis with H_2O_2, apoptotic cells with increased DNA content were distinguishable. A characteristic hypodiploid DNA content peak, which shows sub-G_0/G_1 apoptotic populations, was observed following the treatment of neuronal cells with 7-MH in a concentration-dependent manner (Fig. 3).

To further evaluate the protective molecular mechanisms of 7-MH in neuronal cells, the cells were treated with various concentrations of 7-MH for 2 h, and cell death was induced with H_2O_2 for 4 h. Key proteins involved in apoptosis regulation were examined, including GSK-3, p-p38, Mcl-1, Bcl-2, and BAX, using an immunoblot assay. As demonstrated in Fig. 4, 7-MH markedly inhibited p-p38, BAX, and cleaved caspase-3

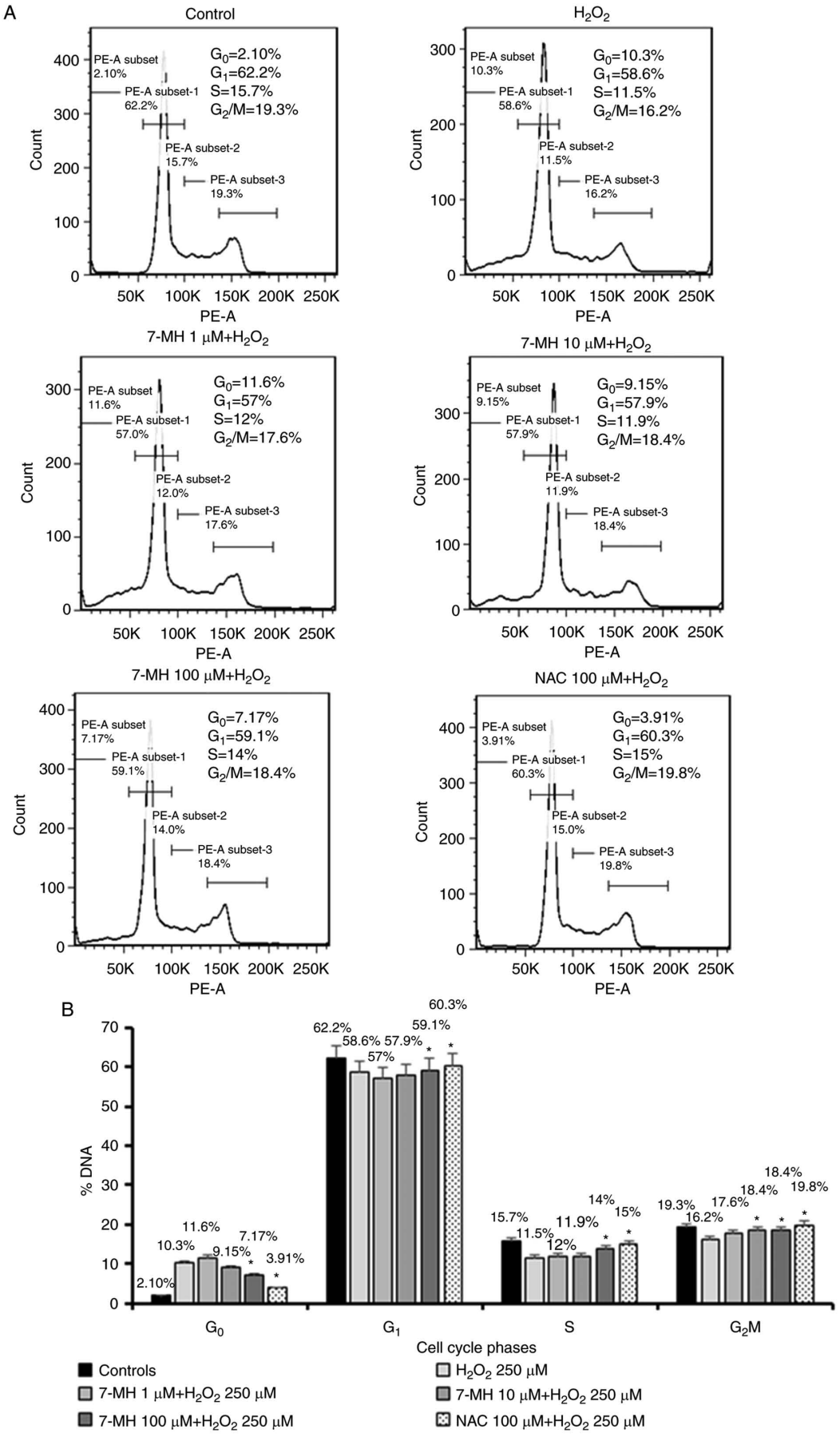

Figure 3. Neuroprotective effect of 7-MH on H_2O_2-induced cell death in neuronal cells. (A and B) Cells were treated with various concentrations of 7-MH and 100 μM NAC (reference compound) for 2 h, and cell death was induced via treatment with a H_2O_2 concentration of 250 μM for 4 h. The cells were then stained with PI and analyzed using flow cytometry. A sub-G_0/G_1 or hypodiploid DNA fraction representing the apoptotic cell population is shown as Ap. 7-MH, 7-methoxyheptaphylline. $^*P<0.05$.

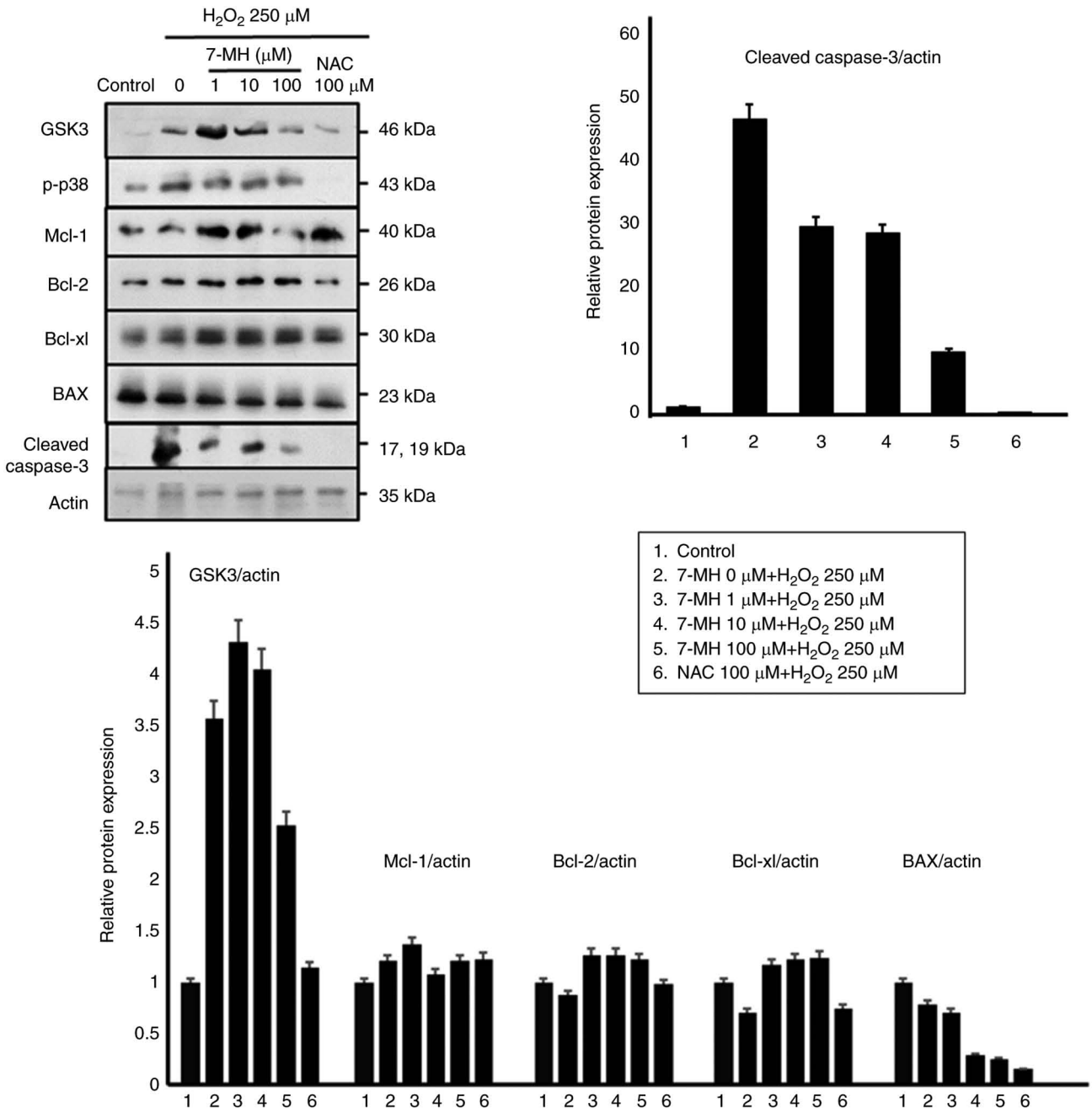

Figure 4. Effect of 7-MH on signaling protein in H_2O_2-induced SHSY-5Y cell apoptosis. Cells were treated with various concentrations of 7-MH for 30 min before switching to 250 μM H_2O_2 for 15 min. Whole-cell extracts were prepared and analyzed by western blotting using anti-caspase-3, GSK-3, p-p38, Mcl-1, Bcl-xL, BAX, Bcl-2, and anti-actin antibodies. 7-MH, 7-methoxyheptaphylline.

compared with the control; and induced Mcl-1, Bcl-2, and Bcl-xL in a concentration-dependent manner. The results indicated that 7-MH efficiently inhibits the apoptotic effect of H_2O_2 induced in neuronal cells.

7-MH induces apoptosis in SH-SY5Y cells via GSK-3. In order to elucidate the molecular mechanism of cancer cellapoptosis, the GSK-3 signaling pathways were assessed. Neuroblastoma cells were treated with various concentrations of 7-MH for 24 h. Cell viability was assessed using MTT assays. These results revealed that 7-MH at a concentration of 100 μM significantly induced cancer cell death with morphological changes, including cell rounding, shrinkage, and detachment (Fig. 5A and B). 7-MH activated the cleaving of caspase-3 by increasing the level of Bax and decreasing the levels of Mcl-1 and Bcl-xl, which are regulated by GSK-3 (Fig. 5C). This indicated that 7-MH induced apoptosis in SH-SY5Y cells via the GSK-3 pathway.

7-MH induces cell death and inhibits migration and invasion of HT29 cancer cells. To test the effect of 7-MH on cancer migration and invasion, HT29 and HepG2 cancer cells were treated with various concentrations of 7-MH for 24 h. Cell viability was assessed using an MTT assay. The results showed that 7-MH at a concentration of 100 μM significantly induced cancer cell death in a time-dependent manner, due to its effect

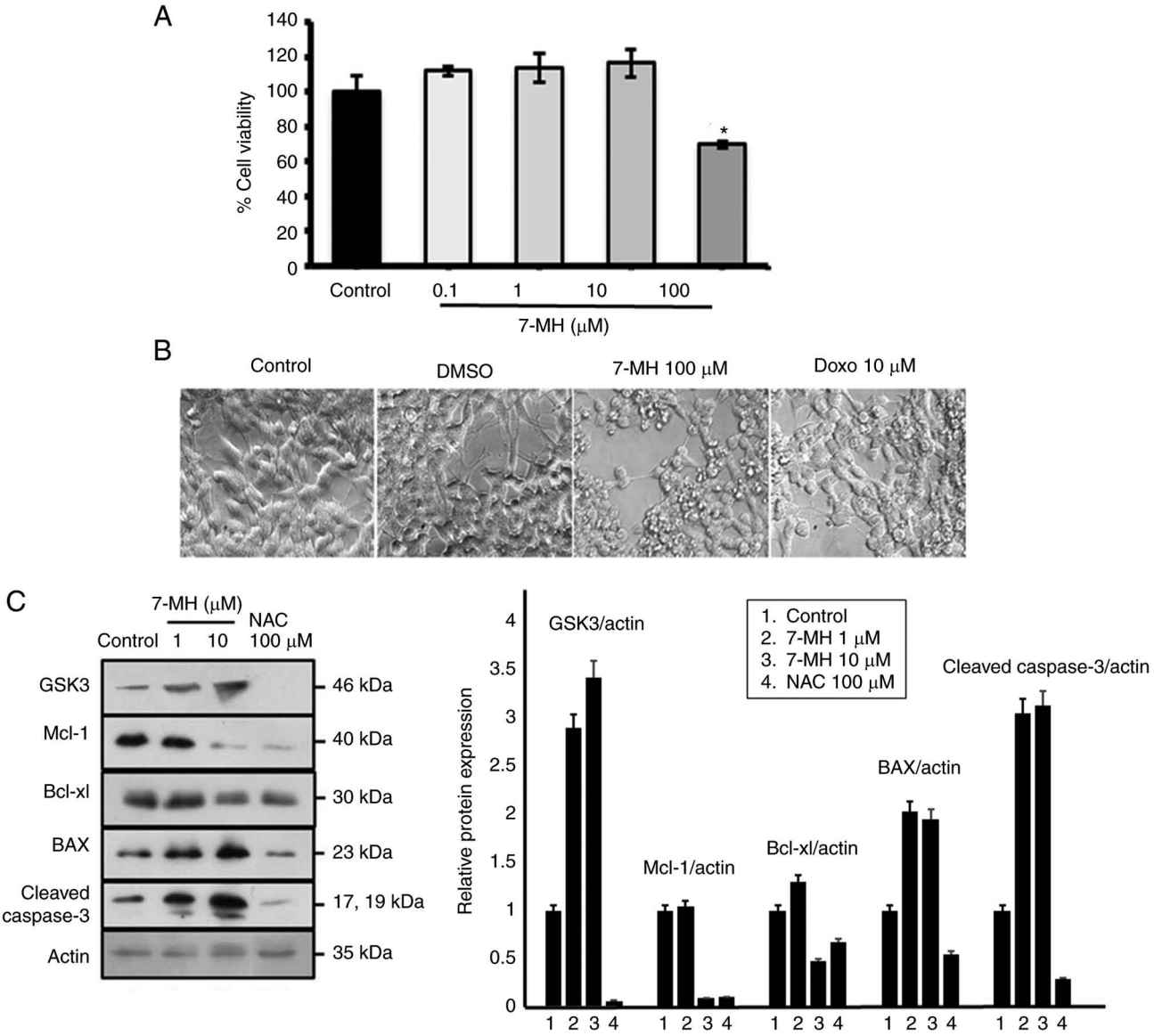

Figure 5. Effect of 7-MH on SHSY-5Y neuroblastoma cell apoptosis. Cells were treated with various concentrations of 7-MH. (A) Cell viability of SHSY-5Y cells treated with 7-MH for 24 h. (B) Cell morphology of SHSY-5Y cells treated with 7-MH for 24 h observed under phase contrast microscopy. (C) Western blot analysis of GSK-3, Mcl-1 Bcl-xl, BAX, cleaved caspase-3, and actin in SHSY-5Y cells treated with 7-MH for 4 h. *P<0.01. 7-MH, 7-methoxyheptaphylline.

on HT29 being more potent than on HepG2 cells (Fig. 6A). The morphological changes, including cell rounding, shrinkage, and detachment, were observed in cells treated with 100 μM of 7-MH compared with 36 μM doxorubicin as a positive control (Fig. 6B). Moreover, 7-MH at concentrations of 1 and 10 μM inhibited the migration and invasion of HT29 cancer cells (Fig. 7A and B). The western blot results revealed that 7-MH activated the cleaving of caspase-3 (marker of apoptosis) and decreased the levels of phospho-Erk, phospho-p38, Bcl-2, survivin, and matrix metalloproteinase-9 (marker of metastasis) (Fig. 8A-C). The results indicated that 7-MH-induced cell death, inhibited migration, and invasion of HT29 cancer cells.

Effects of 7-MH on the viability of LNCaP cells. To examine the effect of 7-MH on the viability of LNCaP cells, the cells were treated with various concentrations of 7-MH for 24, 48 and 72 h, and the cell viability was examined using MTT assay. The result showed that 7-MH significantly inhibited cell growth at concentrations of 1, 10, and 100 μM for 24 h; and at concentrations of 10 and 100 μM for 48 h and 72 h (Fig. 9A). To confirm the effects of 7-MH on LNCaP cell proliferation, cells were treated with various concentrations of 7-MH for 24 h. 7-MH was observed to significantly inhibit cell growth in a dose dependent manner (Fig. 9B). In previous studies, 7-MH was observed to be a carbazole isolated from the roots of *C. harmandiana*, which exhibited cytotoxicity against NCI-H187 (human small-cell lung cancer cells), KB (human epidermoid carcinoma of oral cavity cell lines) and HT29 (human colorectal adenocarcinoma cell line) cells (36-38).

To understand the mechanism by which 7-MH induced cell death, multiple potential signaling pathways that have been demonstrated to be engaged in 7-MH-induced apoptosis were screened. Western blotting showed that 7-MH incubation leads to activation of Akt and p38, whereas the expression of p65, pERK, and MAPK13 was inhibited in a time-dependent

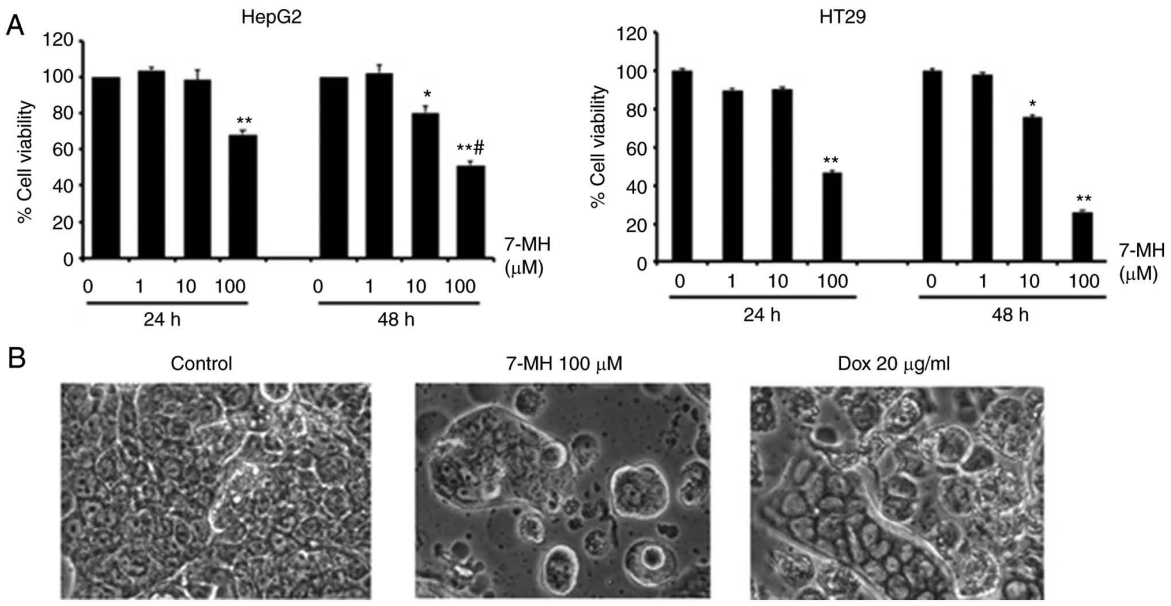

Figure 6. Cytotoxicity of 7-MH to HT-29 and Hep-G2. (A) HT29 and HepG2 cell viability after treatment with 7-MH. (B) HT-29 cell line treatments (control, 7-MH and Dox). *P<0.05, **P<0.01 and #P<0.05 compared with 100 μM 7-MH at 24 h. 7-MH, 7-methoxyheptaphylline; Dox, doxorubicin.

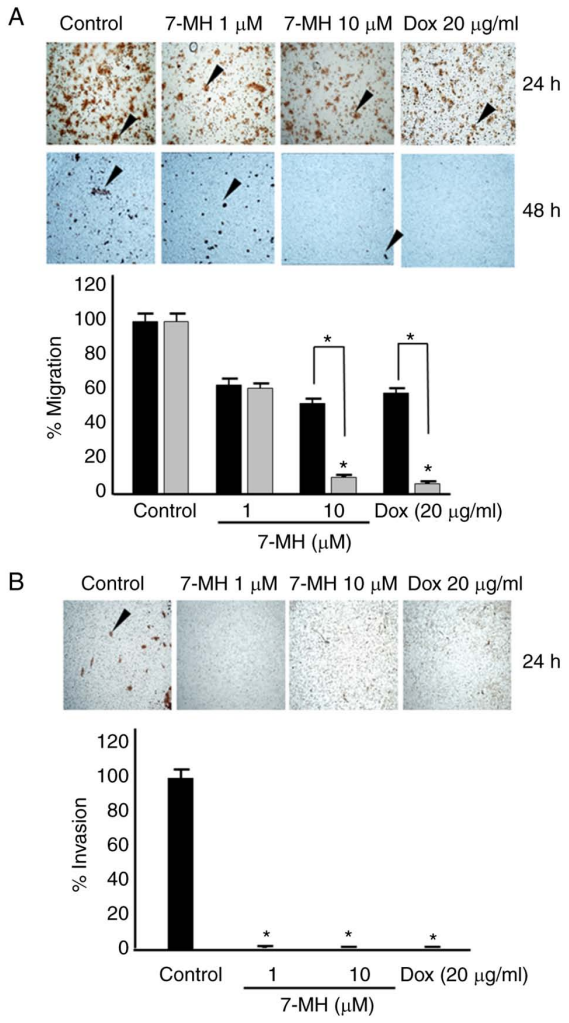

Figure 7. Effects of 7-MH on cancer cell migration and invasion. (A) Results of a Transwell migration assay at 24 and 48 h. (B) A Transwell invasion assay at 24 h in HT-29 after treatment with 7-MH (1 or 10 μM) or Dox (36 μM). *P<0.05. 7-MH, 7-methoxyheptaphylline; Dox, doxorubicin.

manner (Fig. 10). This result indicated that 7-MH induced apoptosis by inducing Akt and p38 activation and inhibiting the p65, pERK, and MAPK13 pathways.

7-MH inhibits the proliferation and metastasis of 4T1 cancer cells. 7-MH significantly reduced the viability of 4T1 cells when compared with resveratrol as a positive control (Fig. 11). The effect of 7-MH on the activation of NF-κB and STAT3 was examined in 4T1 cells stably transfected with an NF-κB- and STAT3-dependent reporter plasmid. Cells were treated with 7-MH for 6 h. It was found that 7-MH inhibited NF-κB and STAT3 activation (Fig. 12).

In 4T1 cancer cell metastasis, the Transwell assay showed that 10 μM of 7-MH significantly inhibited 4T1 cancer cell migration (Fig. 13). *In vivo* assay showed that 7-MH reduced the luminescence signal of 4T1-Luc2 cell metastasis in the lungs of mice (Fig. 14).

The interaction between 7-MH and TAK1 kinase. To understand the binding interactions between 7-MH and TAK1 kinase, a molecular docking study utilizing the Autodock 4.2.6 program was performed. The 4GS6 PDB code, which is bound with the irreversible inhibitor (5Z)-7-oxozeaenol, was used as the TAK1 template. The binding modes and interaction diagrams of 7-MH bound to TAK1 kinase are represented in Fig. 15. The results of docking revealed that 7-MH exhibited multiple binding sites with TAK1 kinase, which are likely to be Lys63, Met104, Tyr106, Ala107, Leu163, Pro160, Cys174, ASP175, Val42, Val50, Val90, Ala61, Gly43, Gly45, Gly110 and Ser111; and its binding energy (ΔG) is-7.72 kcal/mol.

Discussion

In summary, the 7-MH substance is not toxic to neurons, and it can prevent nerve cell death induced by hydrogen peroxide. The Annexin V and PI combined staining is commonly used

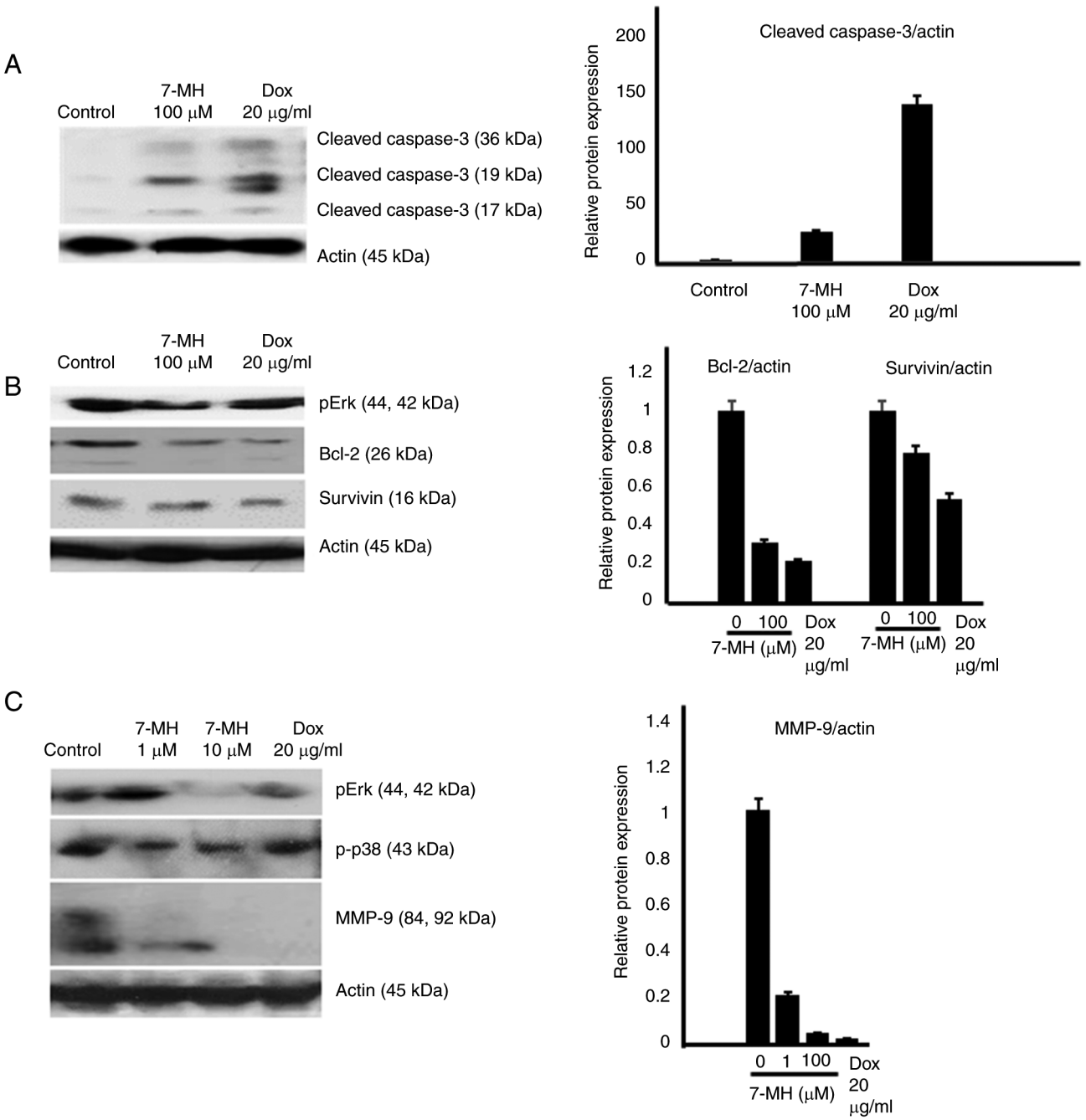

Figure 8. Effects of 7-MH on proteins related to cancer cell apoptosis, migration, and invasion. Cells were treated with various concentrations of 7-MH for 4 h. Whole-cell extracts were prepared and analyzed by western blotting using (A) anti-cleaved caspase-3, (B) phospho-Erk, Bcl-2, survivin and (C) phospho-p38 and MMP-9. Anti-actin antibodies were used as controls. 7-MH, 7-methoxyheptaphylline; Dox, doxorubicin.

for studying the cell cycle. In the present study, there was a limitation to add Annexin V. However, previous studies showed that the PI staining is an also acceptable method to evaluate cell cycle (39-41). Therefore, the cell cycle was investigated by PI staining using flow cytometry. In a previous study by the authors, it was found that 7-MH induced expression of death receptor 5 which plays a role in cell death and is expressed only in cancer cells, but not normal cells, therefore 7-MH induced cell death only in cancer (data not shown). This molecule can inhibit the expression of GSK-3, pp38, BAX, and cleaved caspase-3 proteins, which are apoptosis-related proteins. Moreover, 7-MH increases the expression of proteins that have roles in inhibiting apoptosis, including Bcl-2 and Bcl-xL. It has been showed in previous study that 7-MH is toxic to prostate cancer cells, which can inhibit the expression of the proteins pp65, pERK, and MAPK13. It has been reported that the carbazole from *C. harmandiana* induced apoptosis of HT29 cells (42). The present study showed that 7-MH at 100 μM significantly induces HT-29, Hep-G2 cell, 4T1, and LNCaP cell death (with no significant cytotoxic effects on normal colon cells). Moreover, an inhibitory effect on the migration and invasion of HT29 and 4T1 cancer cells in a concentration and time-dependent manner was observed. Furthermore, it was revealed that 7-MH inhibits cancer proliferation by

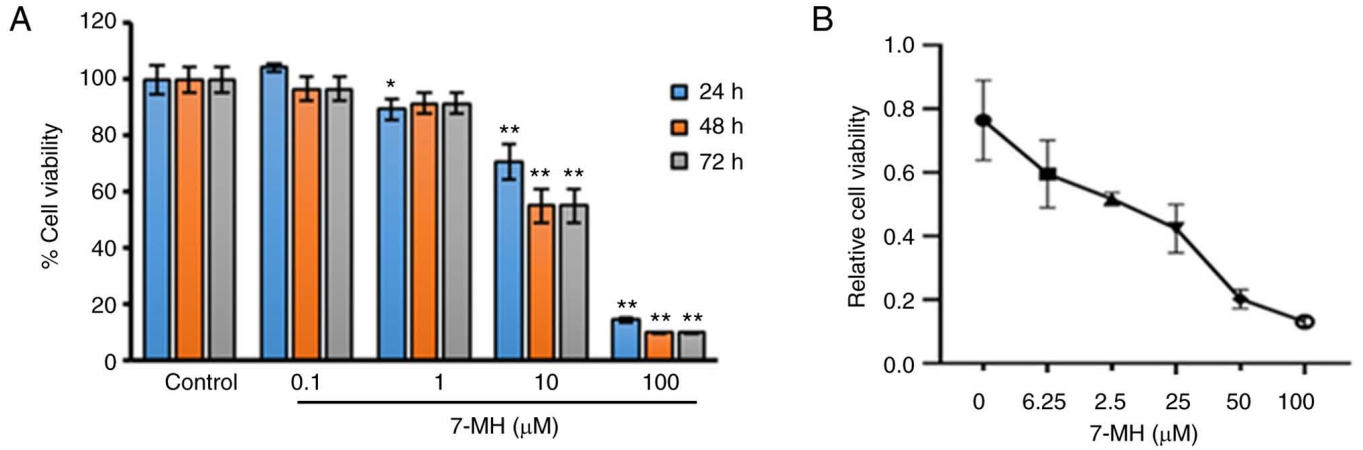

Figure 9. Effect of 7-MH on LNCaP cell death. (A) Cells were treated with 0.1, 1, 10, or 100 μM of 7-MH for 24, 48, or 72 h. (B) Cells were treated with various concentrations of 7-MH for 24 h. *P<0.05 and **P<0.01. 7-MH, 7-methoxyheptaphylline.

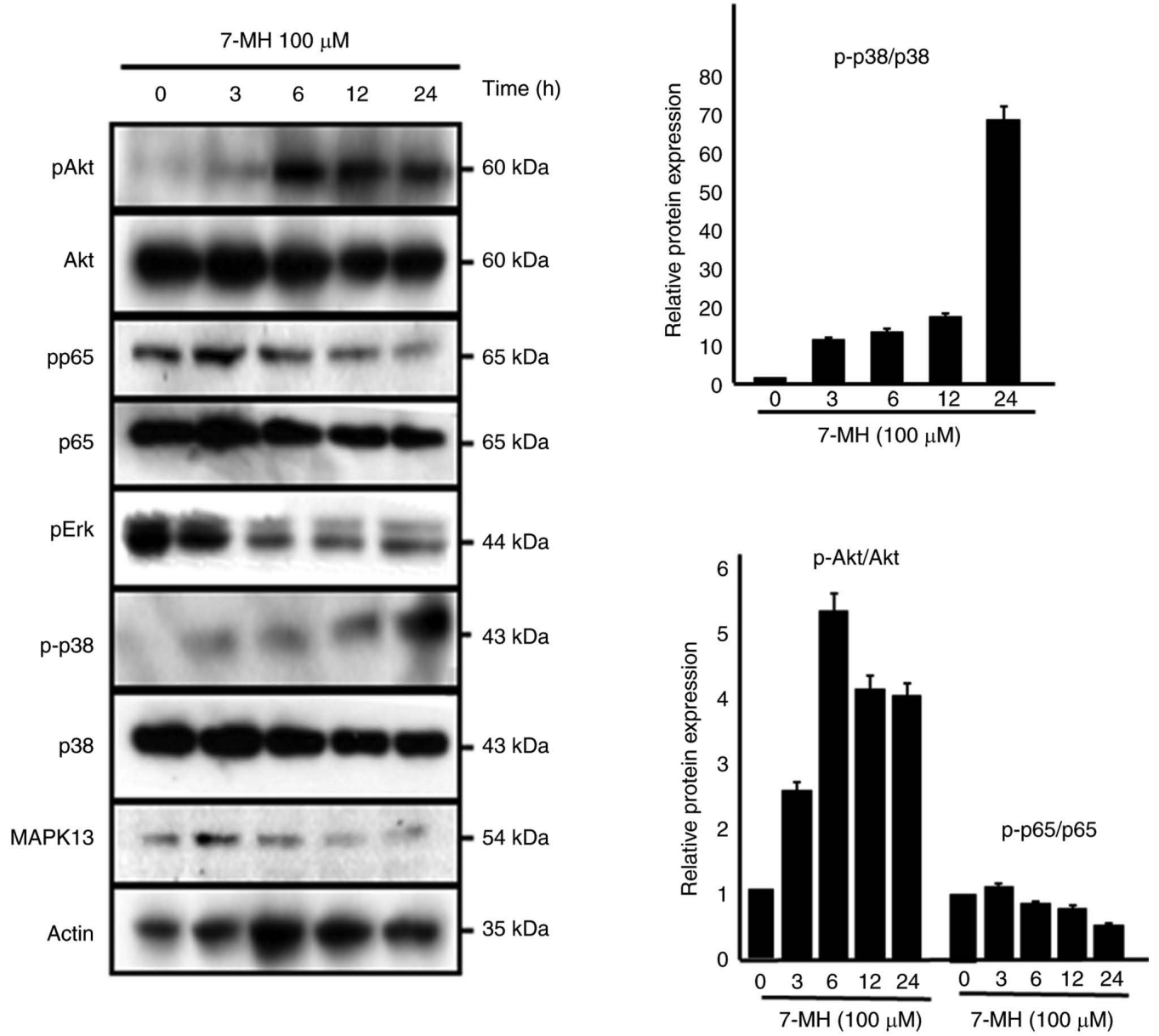

Figure 10. 7-MH-modulated signaling proteins in the LNCaP cell death pathway. Cells were treated with 100 μM of 7-MH for 4 h. Whole-cell extracts were prepared and analyzed by western blotting using anti-phospho-Akt, Akt, phospho-p65, p65, phospho-Erk, phospho-p38, p38, MAPK13, and anti-actin antibodies. 7-MH, 7-methoxyheptaphylline.

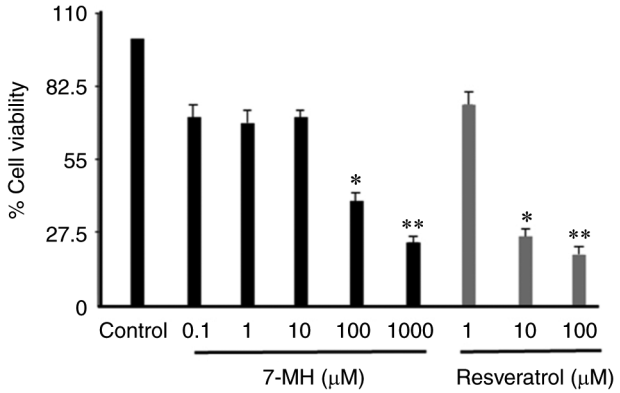

Figure 11. Effect of 7-MH on 4T1 cell death. Cells were treated with DMSO (control) and 0.1, 1, 10, 100, or 1,000 μM of 7-MH for 24 h and compared with resveratrol as a positive control. *P<0.05 and **P<0.01. 7-MH, 7-methoxyheptaphylline.

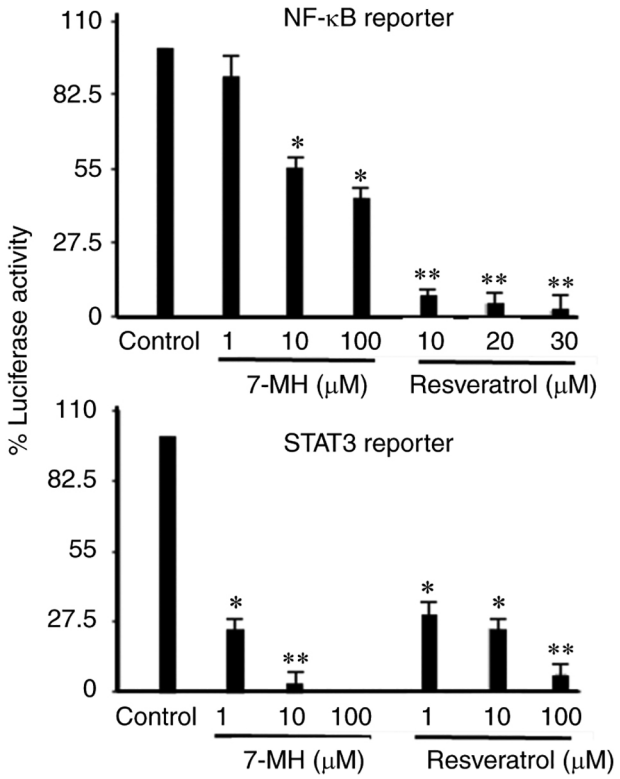

Figure 12. Effect of 7-MH on the activation of NF-κB and STAT3 signaling. 4T1 cells were transfected with NF-κB and STAT3 luciferase reporter plasmids and then treated with DMSO (control) and 0.1, 1, 10, or 100 μM of 7-MH for 24 h and compared with resveratrol as a positive control. *P<0.05 and **P<0.01. 7-MH, 7-methoxyheptaphylline.

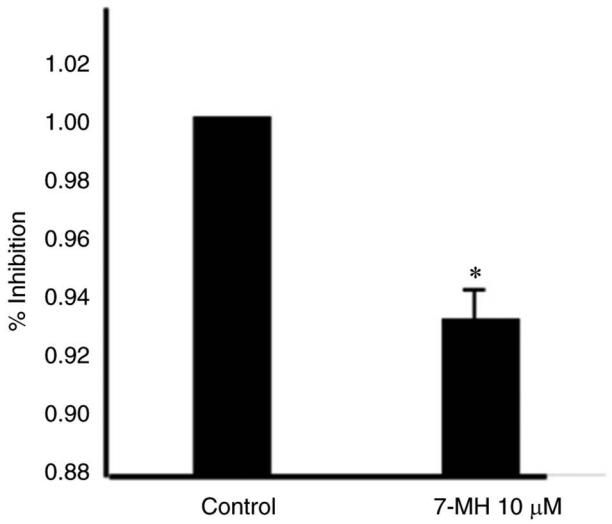

Figure 13. Effect of 7-MH on 4T1 migration. Cells were treated with 10 μM of 7-MH for 24 h, and cell migration was determined using Transwell assay. *P<0.05. 7-MH, 7-methoxyheptaphylline.

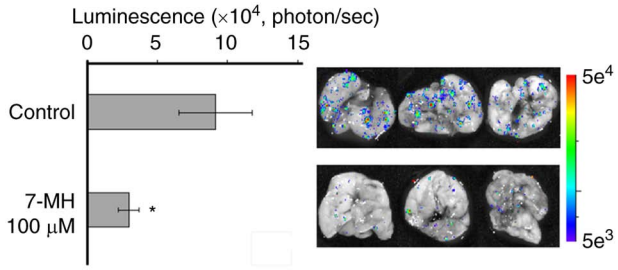

Figure 14. Effect of 7-MH on 4T1-Luc2 cell metastasis in BALB/c mice. 4T1-Luc2 cells were cultured and treated with 0.1% DSMO (control) and 100 μM 7-MH for 48 h; then, mice were inoculated with the cells via intravenous injection, and 2 days after, the lungs were harvested and imaged (n=6 each group). *P<0.05. 7-MH, 7-methoxyheptaphylline.

inhibiting antiapoptotic proteins (Bcl-2, Bcl-xL and survivin) via the MAPK/Erk pathway (Erk1/2), and inhibits the migration and invasion of HT-29, in relation to metastasis of cancer, via MMP-9 inhibition. TAK1, a serine/threonine kinase, acts as a crucial mediator between survival and cell death in TNF-α-mediated signaling. It is an evolutionarily conserved member of the MAP3K family (43). The structure of TAK1 composes of a N terminal (residues 1-104) and C terminal (residues 111-303) domain which are linked together with the hinge region (Met104-Ser111). Lys63 is a key catalytic residue in the active site of TAK1. Asp175 is catalytically important for phosphate transfer to substrate molecules. The hinge region provides an opening for the ATP binding pocket. The purine ring of ATP binds at the hinge region via hydrogen bond forming with Glu105 and Ala107. The ATP also forms hydrogen bond with Asp175 in the DFG motif. The ribose 3'-O of ATP from hydrogen bond with Pro160 (44). The results of docking revealed that 7-MH occupied the ATP-binding pocket of TAK1. 7-MH bound to amino acid residues critical for kinase function: Met104, Tyr106, and Ala107 (hinge region); Lys63 and ASP175 (catalytic amino acid); Pro160 (the binding site of the ribose 3'-O of ATP). Furthermore, 7-MH bound to other amino acid residues including Leu163, Cys174, Val42, Val50, Val90, Ala61, Gly43, Gly45, Gly110 and Ser111. Carbazole ring of 7-MH bound the ATP-binding pocket of TAK1 through: Pi-Pi stacked interaction with Tyr106; Pi-sigma interactions with Val50 and Leu163; Pi-alkyl interactions with Val42, Ala61 and Ala 107; and Pi-sulfur interaction with Met104. The aldehyde and hydroxy substituents on positions 2 and 3, respectively, form hydrogen bonds with ASP175 in the DFG motif. This residue is considered to interact with Lys63 through polar interactions and is catalytically important for phosphate

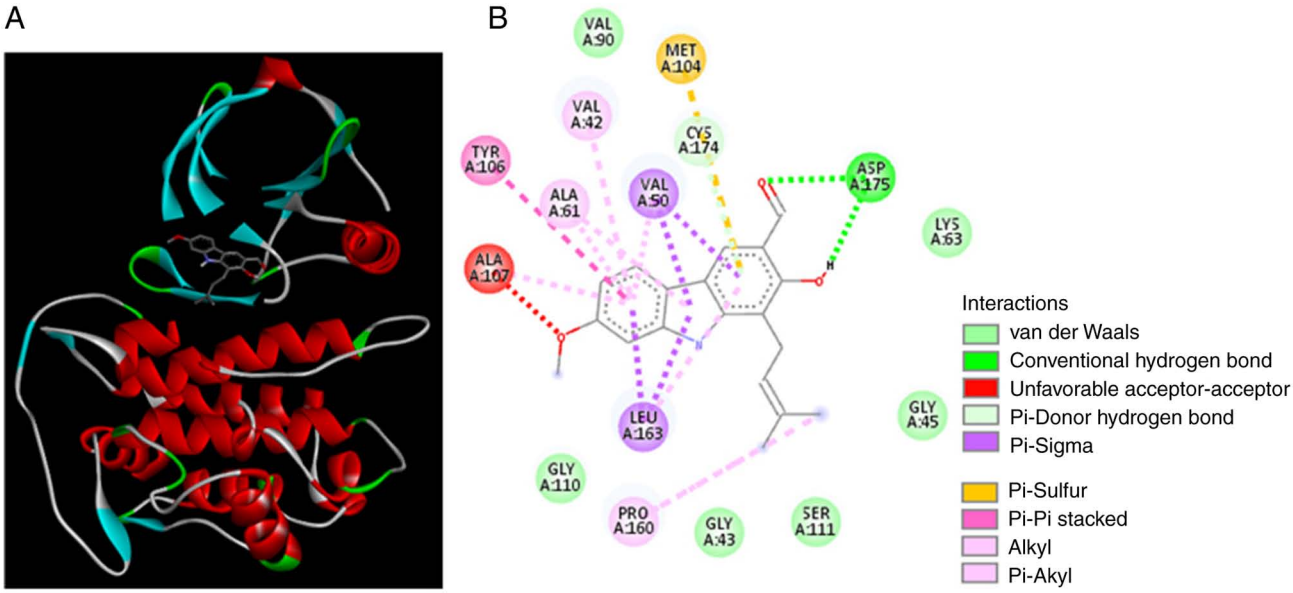

Figure 15. Binding modes (A) and binding interaction diagram (B) of 7-MH bound to TAK1 kinase. Binding interaction between 7-MH and TAK1 kinase (PDB: 4GS6) was performed by using the Autodock 4.2.6 and Discovery studio programs. 7-MH, 7-methoxyheptaphylline; TAK1, transforming growth factor-β (TGF-β)-activated kinase 1.

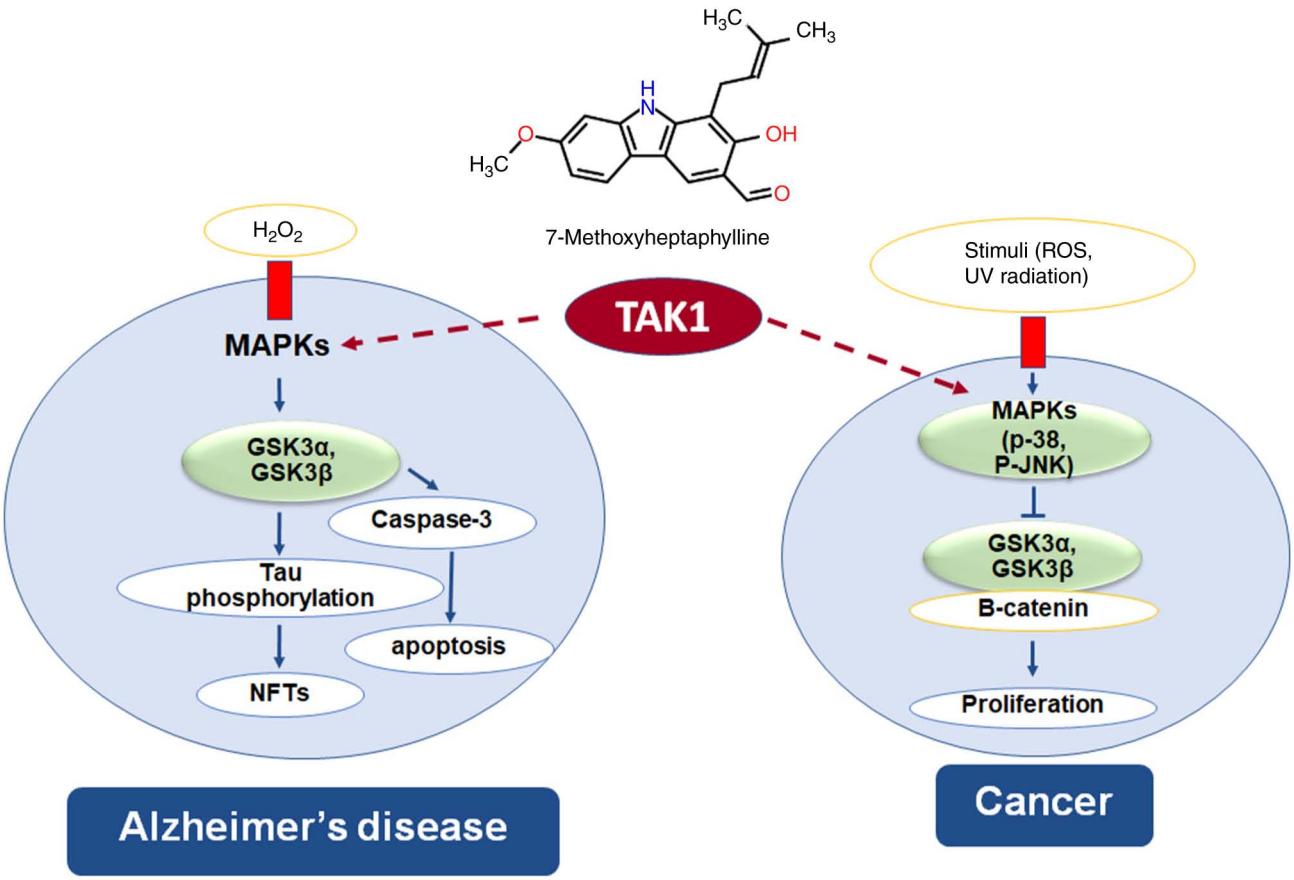

Figure 16. Mechanism of action of 7-MH.

transfer to substrate molecules (45). Moreover, a prenyl group at the position 8 of carbazole ring form hydrophobic interaction with Pro160 which is the key residue target of the ribose 3'-O of ATP. Thus, the docking results confirmed that 7-MH was located in the ATP-binding site, thereby interfering with TAK1 function. In the future study, the interaction between TAK1 and 7-MH will be investigated since in the present study there was a limitation for evaluating TAK1 activity.

GSK-3 is a protein serine/threonine kinase, plays a central role in cellular processes and regulation of disease progression including cancer and AD. In oxidative stress hypothesis of AD, hydrogen peroxide induces neuronal cell death through the MAPKs/GSK-3-mediated apoptosis signaling pathway and GSK-3 also phosphorylates Tau protein to generate neurofibrillary tangles. In cancer cells, β-catenin act as oncoprotein which causes cell proliferation; GSK-3 inhibits β-catenin by phosphorylating β-catenin molecule resulting in degradation of β-catenin (46,47). TAK1 and TAK1-binding protein 1 play an important role in cell apoptosis, migration and invasion through the MAPKs, and NF-κB signal transduction pathways (48). The present study showed that 7-MH has binding site on TAK1 kinase, indicating that 7-MH has neuroprotective effect and anticancer activity via the TAK1 pathway (Fig. 16).

Acknowledgements

Not applicable.

Funding

The present study was supported by the Thailand Research Fund (grant no. TRG5780035), the National Research Council of Thailand and Thailand Research Fund (grant no. DBG6080006), National Science, Research and Innovation Fund, Research Program, Khon Kaen University and the Ubon Ratchathani University of Thailand.

Availability of data and materials

The datasets used and/or analyzed during the current study are available from the corresponding author on reasonable request.

Authors' contributions

PW, CB, CY, YH, PLD and SC conceived the present study. PW, MT, PT and CB developed the methodology and performed formal analysis and investigation. PW and CY provided resources. PW and SC conducted data curation. PW and CB prepared the original draft, wrote, reviewed and edited the manuscript. PW performed project administration. All authors have read and approved the final version of the manuscript. PW and CB confirm the authenticity of all the raw data.

Ethics approval and consent to participate

The animal studies were conducted according to the standard guidelines of the National Institutes of Health and were approved (approval no. A2017INM-7) by the Animal Care and Use Committee of the University of Toyama (Toyama, Thailand).

Patient consent for publication

Not applicable.

Competing interests

The authors declare that they have no competing interests.

References

1. Roe CM, Behrens MI, Xiong C, Miller JP and Morris JC: Alzheimer disease and cancer. Neurology 64: 895-898, 2005.
2. Mattson MP: Cellular actions of beta-amyloid precursor protein and its soluble and fibrillogenic derivatives. Physiol Rev 77: 1081-1132, 1997.
3. Di Luca M, Colciaghi F, Pastorino L, Borroni B, Padovani A and Cattabeni F: Platelets as a peripheral district where to study pathogenetic mechanisms of Alzheimer disease: The case of amyloid precursor protein. Eur J Pharmacol 405: 277-283, 2000.
4. Itoh H, Kataoka H, Koita H, Nabeshima K, Inoue T, Kangawa K and Koono M: Establishment of a new human cancer cell line secreting protease nexin-II/amyloid beta protein precursor derived from squamous-cell carcinoma of lung. Int J Cancer 49: 436-443, 1991.
5. Meng JY, Kataoka H, Itoh H and Koono M: Amyloid beta protein precursor is involved in the growth of human colon carcinoma cell in vitro and in vivo. Int J Cancer 92: 31-39, 2001.
6. Woods NK and Padmanabhan J: Inhibition of amyloid precursor protein processing enhances gemcitabine-mediated cytotoxicity in pancreatic cancer cells. J Biol Chem 288: 30114-30124, 2013.
7. Haven CJ, Howell VM, Eilers PH, Dunne R, Takahashi M, van Puijenbroek M, Furge K, Kievit J, Tan MH, Fleuren GJ, *et al*: Gene expression of parathyroid tumors: Molecular subclassification and identification of the potential malignant phenotype. Cancer Res 64: 7405-7411, 2004.
8. Krause K, Karger S, Sheu SY, Aigner T, Kursawe R, Gimm O, Schmid KW, Dralle H and Fuhrer D: Evidence for a role of the amyloid precursor protein in thyroid carcinogenesis. J Endocrinol 198: 291-299, 2008.
9. Takayama K, Tsutsumi S, Suzuki T, Horie-Inoue K, Ikeda K, Kaneshiro K, Fujimura T, Kumagai J, Urano T, Sakaki Y, *et al*: Amyloid precursor protein is a primary androgen target gene that promotes prostate cancer growth. Cancer Res 69: 137-142, 2009.
10. Takagi K, Ito S, Miyazaki T, Miki Y, Shibahara Y, Ishida T, Watanabe M, Inoue S, Sasano H and Suzuki T: Amyloid precursor protein in human breast cancer: An androgen-induced gene associated with cell proliferation. Cancer Sci 104: 1532-1538, 2013.
11. Miyazaki T, Ikeda K, Horie-Inoue K and Inoue S: Amyloid precursor protein regulates migration and metalloproteinase gene expression in prostate cancer cells. Biochem Biophys Res Commun 452: 828-833, 2014.
12. Hansel DE, Rahman A, Wehner S, Herzog V, Yeo CJ and Maitra A: Increased expression and processing of the Alzheimer amyloid precursor protein in pancreatic cancer may influence cellular proliferation. Cancer Res 63: 7032-7037, 2003.
13. Shiota M, Yokomizo A and Naito S: Pro-survival and anti-apoptotic properties of androgen receptor signaling by oxidative stress promote treatment resistance in prostate cancer. Endocr Relat Cancer 19: R243-R253, 2012.
14. Basu S and Tindall DJ: Androgen action in prostate cancer. Horm Cancer 1: 223-228, 2010.
15. Miyamoto H, Messing EM and Chang C: Androgen deprivation therapy for prostate cancer: Current status and future prospects. Prostate 61: 332-353, 2004.
16. Trachootham D, Alexandre J and Huang P: Targeting cancer cells by ROS-mediated mechanisms: A radical therapeutic approach? Nat Rev Drug Discov 8: 579-591, 2009.
17. Andersen JK: Oxidative stress in neurodegeneration: Cause or consequence? Nat Med 10 (Suppl): S18-S25, 2004.
18. Paravicini TM and Touyz RM: Redox signaling in hypertension. Cardiovasc Res 71: 247-258, 2006.
19. Haigis MC and Yankner BA: The aging stress response. Mol Cell 40: 333-344, 2010.
20. Ray PD, Huang BW and Tsuji Y: Reactive oxygen species (ROS) homeostasis and redox regulation in cellular signaling. Cell Signal 24: 981-990, 2012.
21. Bostwick DG, Alexander EE, Singh R, Shan A, Qian J, Santella RM, Oberley LW, Yan T, Zhong W and Jiang X: Antioxidant enzyme expression and reactive oxygen species damage in prostatic intraepithelial neoplasia and cancer. Cancer 89: 123-134, 2000.
22. Sharifi N, Hurt EM, Thomas SB and Farrar WL: Effects of manganese superoxide dismutase silencing on androgen receptor function and gene regulation: Implications for castration-resistant prostate cancer. Clin Cancer Res 14: 6073-6080, 2008.
23. Khandrika L, Kumar B, Koul S, Maroni P and Koul HK: Oxidative stress in prostate cancer. Cancer Lett 282: 125-136, 2009.

24. Shiota M, Yokomizo A, Tada Y, Inokuchi J, Kashiwagi E, Masubuchi D, Eto M, Uchiumi T and Naito S: Castration resistance of prostate cancer cells caused by castration-induced oxidative stress through Twist1 and androgen receptor overexpression. Oncogene 29: 237-250, 2010.
25. Shiota M, Yokomizo A and Naito S: Oxidative stress and androgen receptor signaling in the development and progression of castration-resistant prostate cancer. Free Radic Biol Med 51: 1320-1328, 2011.
26. Santoro R, Zanotto M, Simionato F, Zecchetto C, Merz V, Cavallini C, Piro G, Sabbadini F, Boschi F, Scarpa A and Melisi D: Modulating TAK1 expression inhibits YAP and TAZ oncogenic functions in pancreatic cancer. Mol Cancer Ther 19: 247-257, 2020.
27. Bang D, Wilson W, Ryan M, Yeh JJ and Baldwin AS: GSK-3α promotes oncogenic KRAS function in pancreatic cancer via TAK1-TAB stabilization and regulation of noncanonical NF-κB. Cancer Discov 3: 690-703, 2013.
28. Santoro R, Carbone C, Piro G, Chiao PJ and Melisi D: TAK-ing aim at chemoresistance: The emerging role of MAP3K7 as a target for cancer therapy. Drug Resist Updat 33-35: 36-42, 2017.
29. Xia S, Ji L, Tao L, Pan Y, Lin Z, Wan Z, Pan H, Zhao J, Cai L, Xu J and Cai X: TAK1 is a novel target in hepatocellular carcinoma and contributes to sorafenib resistance. Cell Mol Gastroenterol Hepatol 12: 1121-1143, 2021.
30. Venna VR, Benashski SE, Chauhan A and McCullough LD: Inhibition of glycogen synthase kinase-3β enhances cognitive recovery after stroke: The role of TAK1. Learn Mem 22: 336-343, 2015.
31. Aouacheria A, Néel B, Bouaziz Z, Dominique R, Walchshofer N, Paris J, Fillion H and Gillet G: Carbazolequinone induction of caspase-dependent cell death in Src-overexpressing cells. Biochem Pharmacol 64: 1605-1616, 2002.
32. Thongthoom T, Songsiang U, Phaosiri C and Yenjai C: Biological activity of chemical constituents from *Clausena harmandiana*. Arch Pharm Res 33: 675-680, 2010.
33. Songsiang U, Thongthoom T, Boonyarat C and Yenjai C: Claurailas A-D, cytotoxic carbazole alkaloids from the roots of *Clausena harmandiana*. Nat J Prod 74: 208-212, 2011.
34. Thiratmatrakul S, Yenjai C, Waiwut P, Vajragupta O, Reubroycharoen P, Tohda M and Boonyarat C: Synthesis, biological evaluation and molecular modeling study of novel tacrine-carbazole hybrids as potential multifunctional agents for the treatment of Alzheimer's disease. Eur J Med Chem 75: 21-30, 2014.
35. Rosini M, Simoni E, Bartolini M, Cavalli A, Ceccarini L, Pascu N, McClymont DW, Tarozzi A, Bolognesi ML, Minarini A, *et al*: Inhibition of acetylcholinesterase, beta-amyloid aggregation, and NMDA receptors in Alzheimer's disease: A promising direction for the multi-target-directed ligands gold rush. J Med Chem 51: 4381-4384, 2008.
36. Kozurkova M, Hamulakova S, Gazova Z, Paulikova H and Kristian P: Neuroactive multifunctional tacrine congeners with cholinesterase, anti-amyloid aggregation and neuroprotective properties. Pharmaceuticals (Basel) 4: 382-418, 2011.
37. Wangboonskul J and Yenjai C: Antioxidant activity and cytotoxicity against cholangiocarcinoma of carbazoles and coumarins from *Clausena harmandiana*. Sci Asia 38: 75-81, 2012.
38. Ghobrial IM, Witzig TE and Adjei AA: Targeting apoptosis pathways in cancer therapy. CA Cancer J Clin 55: 178-194, 2005.
39. Shen Y, Vignali P and Wang R: Rapid profiling cell cycle by flow cytometry using concurrent staining of DNA and mitotic markers. Bio Protoc 7: e2517, 2017.
40. Liu L, Lu Y, Martinez J, Bi Y, Lian G, Wang T, Milasta S, Wang J, Yang M, Liu G, *et al*: Proinflammatory signal suppresses proliferation and shifts macrophage metabolism from Myc-dependent to HIF1α-dependent. Proc Natl Acad Sci USA 113: 1564-1569, 2016.
41. Riccardi C and Nicoletti I: Analysis of apoptosis by propidium iodide staining and flow cytometry. Nat Protoc 1: 1458-1461, 2006.
42. Boonyarat C, Yenjai C, Vajragupta O and Waiwut P: Heptaphylline induces apoptosis in human colon adenocarcinoma cells through bid and Akt/NF-κB (p65) pathways. Asian Pac J Cancer Prev 15: 10483-10487, 2014.
43. Manning G, Whyte DB, Martinez R, Hunter T and Sudarsanam S: The protein kinase complement of the human genome. Science 298: 1912-1934, 2002.
44. Totzke J, Scarneo SA, Yang KW and Haystead TAJ: TAK1: A potent tumour necrosis factor inhibitor for the treatment of inflammatory diseases. Open Biol 10: 200099, 2020. Brown K, Vial SCM, Dedi N, Long JM, Dunster NJ and Cheetham GMT: Structural basis for the interaction of TAK1 kinase with its activating protein TAB1. J Mol Biol 354: 1013-1020, 2005.
45. Mancinelli R, Carpino G, Petrungaro S, Mammola CL, Tomaipitinca L, Filippini A, Facchiano A, Ziparo E and Giampietri C: Multifaceted roles of GSK-3 in cancer and autophagy-related diseases. Oxid Med Cell Longev 2017: 4629495, 2017.
46. Rippin I and Eldar-Finkelman H: Mechanisms and therapeutic implications of GSK-3 in treating neurodegeneration. Cells 10: 262, 2021.
47. Kyriakis JM and Avruch J: Mammalian MAPK signal transduction pathways activated by stress and inflammation: A 10-year update. Physiol Rev 92: 689-737, 2012.

This work is licensed under a Creative Commons Attribution-NonCommercial 4.0 International (CC BY-NC 4.0) License.